CHIN. PHYS. LETT. Vol. 32, No. 7 (2015) 077401

Doping Induced Gap Anisotropy in Iron-Based Superconductors: a Point-Contact Andreev Reflection Study of $BaFe_{2-x}Ni_xAs_2$ Single Crystals *

ZHU Jun(朱军)[1], WANG Zhao-Sheng(王钊胜)[1], WANG Zhen-Yu(王震宇)[1], HOU Xing-Yuan(侯兴元)[1], LUO Hui-Qian(罗会仟)[1], LU Xing-Ye(鲁兴业)[1], LI Chun-Hong(李春红)[1], SHAN Lei(单磊)[1], WEN Hai-Hu(闻海虎)[2], REN Cong(任聪)[1]**

[1]*National Laboratory for Superconductivity, Institute of Physics and Beijing National Laboratory for Condensed Matter Physics, Chinese Academy of Sciences, Beijing 100190*

[2]*Department of Physics, Nanjing University, Nanjing 210093*

(Received 16 April 2015)

We report a systematic investigation on c-axis point-contact Andreev reflection (PCAR) in $BaFe_{2-x}Ni_xAs_2$ superconducting single crystals from underdoped to overdoped regions ($0.075 \leq x \leq 0.15$). At low temperatures, an in-gap sharp peak at low-bias voltage is observed in PCAR for overdoped samples, in contrast to the case of underdoped junctions, in which an in-gap plateau is observed. The variety of the conductance spectra with doping can be well described by using a generalized Blonder–Tinkham–Klapwijk formalism with an angle-dependent gap. This gap shows a clear crossover from a nodeless in the underdoped side to a nodal feature in the overdoped region. This result provides evidence of the doping-induced evolution of the superconducting order parameter when the inter-pocket and intra-pocket scattering are tuned through doping, as expected in the $s_\pm$ scenario.

PACS: 74.20.Rp, 74.25.Ha, 74.70.Dd DOI: 10.1088/0256-307X/32/7/077401

Among the unsettled issues of the iron pnictide superconductivity, the pairing symmetry of its superconducting gap is the most important to address. It is generally accepted that superconductivity in iron pnictides results from a superexchange repulsion mediated by magnetic excitations, which couples electron and hole pockets of the Fermi surface.[1–3] Such pairing interactions favor either isotropic s-wave order parameters with opposite signs on different sheets of the Fermi surface ($s\pm$ model) or anisotropic s-wave or d-wave order parameters with nodes.[4,5] Consensus has been reached on several systems, e.g., LaFePO,[6] KFe_2As_2,[7] $BaFe_2(As_{1-x}P_x)_2$,[8] where nodes exist on the gap structure. However, experimental confirmations of such a nodal-gap state remains highly controversial in other systems.[9–19,21] For example, measurements of the electronic specific heat of $Ba(Fe_{1-x}Co_x)_2As_2$ have shown a field dependence consistent with both a fully gapped FS[12] and a nodal quasiparticals at the Fermi level.[16,17] Such scattered experimental results and interpretations may come from the different qualities and doping level of the samples studied. Discovering the evolution of the Fermi surface as a function of the various material parameters which drive the material from an underdoped antiferromagnetic spin density wave (SDW) state, through the superconducting dome and eventually towards an overdoped paramagnetic metal, should therefore be an important step towards a complete understanding of the mechanism that drives high temperature superconductivity in these materials.

$BaFe_2As_2$ (122) stands out among the members of iron-pnictide series due to its diverse superconductivity. As potassium partially substitutes Ba, 122 becomes hole-doped $Ba_{1-x}K_xFe_2As_2$ superconductors. On the other hand, Co/Ni dopes into the Fe site, and 122 becomes electron-doped $Ba(Fe_{1-x}Ni(Co)_x)_2As_2$. For hole-doped $Ba_{1-x}K_xFe_2As_2$ superconductors, it has been proven in experiment that a nodeless $s_\pm$-wave superconducting state is dominant for an optimally doped compound.[18,19] However, it is argued that a nodal s-wave or even d-wave state is dominant for extremely over-doped KFe_2As_2.[20,21] Such an evolution of pairing symmetry with doping level has not been investigated for electron-doped compounds.

Point-contact Andreev reflection(PCAR) spectroscopy has been adopted for probing the density of state (DOS) of superconductors with the high energy resolution. In addition, the capability of this technique to study the anisotropy and the temperature dependence of the superconducting gap make it a unique tool in providing invaluable information for various mechanisms of unconventional superconductivity (for a review, see Refs. [22,23]). Several theoretical calculations have been reported on the PCAR conductance characteristics of a junction involving the $s_\pm$ symmetry in iron pnictide superconductors.[24,25] In this Letter, we fabricate highly transparent *c*-axis direct contacts to perform the PCAR spectroscopy study on a series of electron-doped $BaFe_{2-x}Ni_xAs_2$ single crys-

*Supported by the National Basic Research Program of China under Grant Nos 2011CBA00100 and 2012CB821404, and the Project of International Team on Superconductivity and Novel Electronic Materials of Chinese Academy of Sciences.

**Corresponding author. Email: cong_ren@iphy.ac.cn

tals over a wide doping range. The conductance spectra show a systematic and consistent behavior with the variation of the doping level, indicating a doping dependence of the order parameter for Ni-122 superconductors.

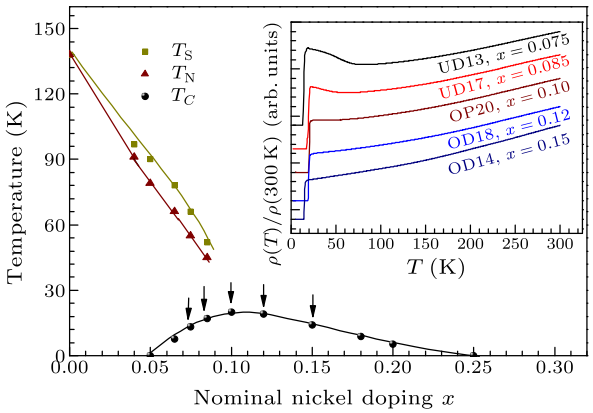

Fig. 1. (Color online) Phase diagram of $BaFe_{2-x}Ni_xAs_2$ as a function of Ni concentration x. The orthorhombic phase below T_s and the antiferromagnetic (AF) phase below T_N are also shown here. The arrows indicate the doping levels of the samples under investigation. Inset: temperature dependence of the in-plane resistivity ρ for the samples with the Ni nominal doping level x as labeled. The data are vertically shifted for clarity.

High-quality single crystals of $BaFe_{2-x}Ni_xAs_2$ were grown from a self-flux method, as described elsewhere.[26] The crystals were characterized by using x-ray diffraction and energy dispersion (EDX). The doping level in the crystals was determined by inductive coupled plasma emission spectrometer (ICP), which gave a Ni concentration roughly 0.8 times the nominal content x. We choose five compositions: underdoped, $x = 0.075$ (UD13), 0.085 (UD17); overdoped, with $x = 0.12$ (OD18), 0.15 (OD14), and optimally doped with $x = 0.1$ (OP20). The typical level of impurity phases has been checked by specific heat measurement on the optimally doped crystal $x = 0.1$, in which a residual component γ_0 at $T \to 0$ revealed an impurity phase of ~4%.[27] The temperature dependence of resistivity for these five compositions under investigation is displayed in the inset of Fig. 1, by which the bulk transition temperature T_c is determined (95% of the normal state resistivity) for each composition. Consequently, the T_c value for each composition is shown on the phase diagram in the main panel of Fig. 1.

Point contacts to the flat and shiny surfaces cleaved along the c-axis of $BaFe_{2-x}Ni_xAs_2$ crystals were made by using thick silver paste bonding with gold wires. The typical size of these planar contacts is about 80–150 μm under a microscope. Due to the nanocrystalline nature of the silver paint, the contact made in this way is actually formed by many nanocontacts analogue to the tip point-contact technique.[23] For the backside electrical wiring, we applied ultrapure indium or silver paste to cover the whole area of the bottom surfaces of the crystals. The contacts made in this way remain stable in thermal cycling, and the contact resistance at high bias R_N varies slightly (<6 over the whole T range up to T_c, indicating that there is no excess conductance (resistance) involved in the junction conductance (resistance).

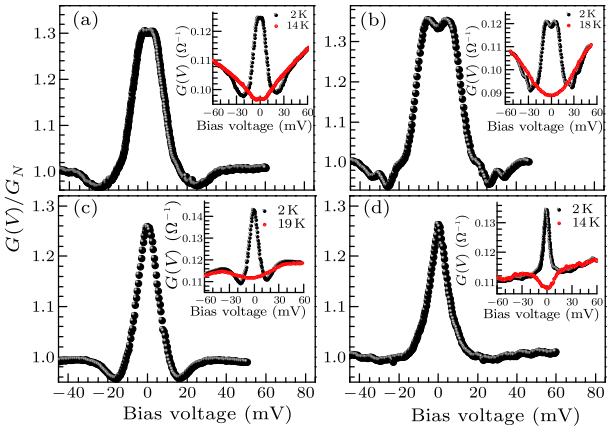

Fig. 2. (Color online) The normalized conductance spectrum $G(V)/G_N$ at $T = 2$ K with G_N the conductance spectrum of normal state background for (a) UD13, (b) UD17, (c) OD18 and (d) OD14. Inset: the corresponding raw data of conductance spectra at 2 K and above T_c (the red dots) for comparison, respectively.

We have measured the point-contact $G(V)$ curves in the whole T range up to T_c for junctions with $x = 0.075$ (UD13), 0.085 (UD17), 0.12 (OD18), and 0.15 (OD14). The typical $G(V)$ curves at T=2 K ($< 0.2T_c$) and $T \geq T_c$ are shown in Figs. 2(a)–2(d). As shown, these $G(V)$ curves exhibit a consistent behavior. (i) An underlying feature of a dominant single gap is unambiguously identified with a similar conductance enhancement of 25%–30% for each junction. (ii) A parabolic normal-state $G(V)$ curve with a slight asymmetry at $T \geq T_c$ for each x, opposite to those of hole-doped K-122,[28,29] implies the similar origin of the underlying normal-state background. Nevertheless, a striking feature in these normalized (and the raw) $G(V)$ curves is that: at $T = 2$ K, a conductance plateau and/or a double peak around zero bias for junctions UD13 and UD17 gradually evolves into an in-gap sharp peak in $G(V)$ for junctions OD18 and OD14. Considering the overall spectral consistency in these junctions, the systematic evolution of the Andreev conductance spectra with doping concentration is nontrivial. Qualitatively, for highly transparent junctions at finite T, the appearance of an in-gap plateau in the Andreev conductance spectrum is a signature of a fully gapped state. In contrast, an in-gap conductance peak is a characteristic of an anisotropic gap state due to the presence of a finite DOS at low energy, like a d-wave gap in cuprates.[22]

To explicitly describe the variety of spectral behavior observed and quantitatively resolve the gap amplitude, we invoke a generalized Blonder–Tinkham–Klapwijk (BTK) formula[31] with three parameters: a dimensionless parameter Z which represents the interface transparency; an imaginary quasiparticle energy modification Γ[32] which reflects the spectral broadening, and the superconducting gap Δ. In the BTK model, the Andreev reflection and normal probabilities, A and B, respectively, are related to the DOS of the superconductor $N_s = N_0 \mathrm{Re}(\frac{E-i\Gamma}{\sqrt{(E-i\Gamma)^2-\Delta^2(T,\theta)}})$ with N_0 the normal-state DOS and θ the crystalline angle parallel to the current injection. To choose a gap function to calculate these conductance spectra, we assume, based on the $s_\pm$ scenario, an anisotropic gap of the general form $\Delta_0|1-r+r\cos(2\theta)|$, with the gap anisotropy ratio r varying from r=0 (isotropic $s_\pm$ state) to r=1 (completely nodal gap).[33,34] We note that it is not easy to describe the spectral behavior using a simple formulism, due to the fact that we are dealing with a multi-band or/and even multi-gap system.

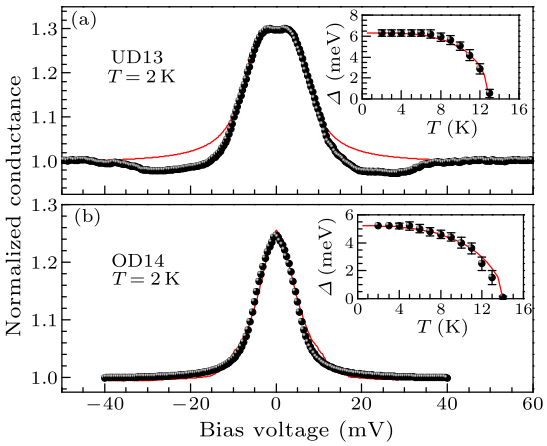

Fig. 3. Normalized conductance curves at $T = 2$ K for c-axis contacts: (a) UD13 and (b) OD14. The red solid lines are their single effective-gap fits with the relevant fitting parameters. Insets: the obtained superconducting gaps Δ as a function of T for UD13 (a) and OD14 (b). The solid lines are their fits to an empirical α gap function.

Examples of normalized $G(V)$ curves and their fits at $T = 2$ K are shown in the main panels of Figs. 3(a) and 3(b) for junctions UD13 and OD14, respectively. The single effective-gap BTK model (red lines) fit very well with the main features of the experimental $G(V)$ curves, yielding a set of fitting parameters associated with gap magnitude and anisotropy ratio: $\Delta_0 = 6.2$ meV and $r = 0$ for UD13 and $\Delta_0 = 5.3$ meV and $r = 1$ for OD14, respectively. It is noted that the same gap magnitude is also extracted from a recent PCAR experiment on a c-axis $Ag/BaFe_{1.8}Co_{0.2}As_2$ with the comparable $T_c = 24$ K.[28] With these fitting parameters, we check the validity of these fits by extending the fit to the overall temperature spectral to extract $\Delta(T)$ functions. In this overall-T spectral fit (not shown here), $r = 0$ and $Z = 0.48$–0.52, $\Gamma_h = 2.7$ meV are constant with T for UD13 while $r = 1$, $Z = 0.32$–0.36, and $\Gamma = 2.3$ meV for the OD14 sample. From the fits, we obtain a BCS-like Δ–T dependence, which is plotted in Figs. 3(a) and 3(b) for both the junctions, respectively. For comparison, the obtained gaps can be approximated by an empirical gap formula: $\Delta(T) = \Delta_0 \tanh(\alpha\sqrt{T_c/T-1})$ with $\alpha = 2.2$ for UD13 and 2.06 for OD14 ($\alpha = 1.74$ for weak-coupling BCS gap), both in the strong coupling limit.

We analyze the physical meanings of the obtained gap anisotropy and gap function from our fitting. The obtained anisotropy ratio $r = 0$, resolved in our c-axis PCAR spectroscopy of underdoped crystals, indicates a fully-gapped state along c axis. On the contrary, $r = 1$ in overdoped crystals means an extremely anisotropic gap or even a nodal gap for overdoped compounds. This crossover of nodeless $s_\pm$-wave to nodal s-wave states occurs around optimally doped Ni-122 samples. This situation of the $BaFe_{1-x}Ni_xAs_2$ system is similar to that of optimally doped Co-122, in which a gap minima is already present at the maximal T_c along the c-axis.[35,36] Therefore, our observation of the systematic evolution from the in-gap conductance plateau for the underdoped samples to the in-gap peak in the $G(V)$ curves for the overdoped samples indicates the existence of doping induced evolution of superconducting gaps with an isotropic feature in the underdoped region to an anisotropic, even, nodal gap in the overdoped side. This is highly consistent with the result of the T-dependent penetration depth λ in a series of Ni-122 superconductors, in which $\Delta\lambda \propto T^n$ with the exponent $n \geq 2$ for underdoped samples and $\Delta\lambda$ becomes more linear-T dependent for overdoped samples, indicating the development of nodal gaps in the overdoped region.[14]

In summary, we have fabricated point-contact junctions on high quality single crystals of $BaFe_xNi_{1-x}As_2$ to perform Andreev conductance spectral measurements. The Andreev conductance spectra clearly show a full-gap state for underdoped crystals and a highly anisotropic, even nodal-like gap state for overdoped crystals. Quantitative analysis by using a generalized BTK formalism with an angle-dependent gap can well describe these changes of doping-dependent spectral behaviors. Resulting from the analytical fitting, the gap shows a clear crossover from a nodeless in the underdoped side to a nodal feature in the overdoped region. This result provides evidence of the doping-induced evolution of the superconducting order parameter when the inter-pocket and intra-pocket scattering are tuned through doping, consistent with the band structure calculation

which is based on a strong-coupling spin fluctuation approach.

We are grateful to Prozorov R., Wang Q. H. and Li S. L. for intensive discussions.

References

[1] Mazin I I, Singh D J, Johannes M D and Du M H 2008 *Phys. Rev. Lett.* **101** 057003
[2] Wang F, Zhai H, Ran Y, Vishwanath A and Lee D H 2009 *Phys. Rev. Lett.* **102** 047005
[3] Kuroki K, Onari S, Arita R, Usui H, Tanaka Y, Kontani H and Aoki H 2008 *Phys. Rev. Lett.* **101** 087004
[4] Kuroki K, Usui H, Onari S, Arita R and Aoki H 2009 *Phys. Rev.* B **79** 224511
[5] Graser S, Kemper A F, Maier T A, Cheng H P, Hirschfeld P J and Scalapino D J 2010 *Phys. Rev.* B **81** 214503
Maier T A, Graser S, Scalapino D J and Hirschfeld P J 2009 *Phys. Rev.* B **79** 224510
[6] Fletcher J D, Serafin A, Malone L, Analytis J G, Chu J H, Erickson A S, Fisher I R and Carrington A 2009 *Phys. Rev. Lett.* **102** 147001
Hicks C W, Lippman T M, Huber M E, Analytis J G, Chu J H, Erickson A S, Fisher I R and Moler K A 2009 *Phys. Rev. Lett.* **103** 127003
[7] Dong J K, Zhou S Y, Guan T Y, Zhang H, Dai Y F, Qiu X, Wang X F, He Y, Chen X H and Li S Y 2010 *Phys. Rev. Lett.* **104** 087005
Hashimoto K, Serafin A, Tonegawa S, Katsumata R, Okazaki R, Saito T, Fukazawa H, Kohori Y, Kihou K, Lee C H, Iyo A, Eisaki H, Ikeda H, Matsuda Y, Carrington A and Shibauchi T 2010 *Phys. Rev.* B **82** 014526
[8] Hashimoto K, Yamashita M, Kasahara S, Senshu Y, Nakata N, Tonegawa S, Ikada K, Serafin A, Carrington A, Terashima T, Ikeda H, Shibauchi T and Matsuda Y 2010 *Phys. Rev.* B **81** 220501(R)
[9] Ding H, Richard P, Nakayama K, Sugawara K, Arakane T, Sekiba Y, Takayama A, Souma S, Sato T, Takahashi T, Wang Z, Dai X, Fang Z, Chen G F, Luo J L and Wang N L 2008 *Europhys. Lett.* **83** 47001
[10] Wang Q Y, Li Z, Zhang W H, Zhang Z C, Zhang J S, Li W, Ding H, Ou Y B, Deng P, Chang K, Wen J, Song C L, He K, Jia J F, Ji S H, Wang Y Y, Wang L L, Chen X, Ma X C and Xue Q K 2012 *Chin. Phys. Lett.* **29** 037402
[11] Zhang X H, Oh Y S, Liu Y, Yan L Q, Kim K H, Greene R L and Takeuchi I 2009 *Phys. Rev. Lett.* **102** 147002
Zhang X H, Oh Y S, Liu Y, Yan L Q, Saha S R, Butch N P, Kirshenbaum K, Kim K H, Paglione J, Richard Greene L and Takeuchi I 2010 *Phys. Rev.* B **82** 020515(R)
[12] Hardy F, Ademann P, Wolf T, Löhneysen H V and Meingast C 2009 *Phys. Rev. Lett.* **102** 187004
[13] Reid J P, Tanatar M A, Luo X G, Shakeripour H, Doiron-Leyraud N, Ni N, Bud'ko S L, Canfield P C, Prozorov R and Taillefer L 2010 *Phys. Rev.* B **82** 064501
[14] Prozorov R, Tanatar M A, Ni N, Kreyssig A, Nandi S, Bud'ko S L, Goldman A I and Canfield P C 2009 *Phys. Rev.* B **80** 174517
[15] Martin C, Kim H, Gordon R T, Ni N, Kogan V G, Bud'ko S L, Canfield P C, Tanatar M A and Prozorov R 2010 *Phys. Rev.* B **81** 060505(R)
[16] Gofryk K, Vorontsov A B, Vekhter I, Sefat A S, Imai T, Bauer E D, Thompson J D and Ronning F 2011 *Phys. Rev.* B **83** 064513
[17] Mu G, Tang J, Tanabe Y, Xu J T, Heguri S and Tanigaki K 2011 *Phys. Rev.* B **84** 054505
[18] Ren C, Wang Z S, Luo H Q, Yang H, Shan L and Wen H H 2008 *Phys. Rev. Lett.* **101** 257006
[19] Shan L, Wang Y L, Gong J, Shen B, Huang Y, Yang H, Ren C and Wen H H 2011 *Phys. Rev.* B **83** 060510(R)
[20] Xu N, Richard P, Shi X, Roekeghem A V, Qian T, Razzoli E, Rienks E, Chen G F, Ieki E, Nakayama K, Sato T, Takahashi T, Shi M and Ding H 2013 *Phys. Rev.* B **88** 220508(R)
[21] Tafti F F, Juneau F A, Delage M, Renè de Cotret S, Reid J P, Wang A F, Luo X G, Chen X H, Doiron L N and Taillefer L 2013 *Nat. Phys.* **9** 349
[22] Deutscher G 2005 *Rev. Mod. Phys.* **77** 109
[23] Daghero D and Gonnelli R S 2010 *Supercond. Sci. Technol.* **23** 043001
[24] Golubov A A, Brinkman A, Tanaka Y, Mazin I I and Dolgov O V 2009 *Phys. Rev. Lett.* **103** 077003
Ghaemi P, Wang F and Vishwanath A 2009 *Phys. Rev. Lett.* **102** 157002
[25] Wang D, Wan Y and Wang Q H 2009 *Phys. Rev. Lett.* **102** 197004
Sperstad I B, Linder J and Sudbø A 2009 *Phys. Rev.* B **80** 144507
Araújo M A N and Sacramento P D 2009 *Phys. Rev.* B **79** 174529
[26] Chen Y C, Lu X Y, Wang M, Luo H Q and Li S L 2011 *Supercond. Sci. Technol.* **24** 065004
[27] Zeng B, Mu G, Shen B, Cheng P, Luo H Q, Yang H, Shan L, Ren C and Wen H H 2012 *Phys. Rev.* B **85** 224514
[28] Tortello M, Daghero D, Ummarino G A, Stepanov V A, Jiang J, Weiss J D, Hellstrom E E and Gonnelli R S 2010 *Phys. Rev. Lett.* **105** 237002
[29] Lu X, Park W K, Yuan H Q, Chen G F, Luo G L, Wang N L, Sefat A S, McGuire M A, Jin R, Sales B C, Mandrus D, Gillett J, Sebastian S E and Greene L H 2010 *Supercond. Sci. Technol.* **23** 054009
[30] Blonder G E, Tinkham M and Klapwijk T M 1982 *Phys. Rev.* B **25** 4515
[31] Tanaka Y and Kashiwaya S 1995 *Phys. Rev. Lett.* **74** 3451
Kashiwaya S, Tanaka Y, Koyanagi M and Kajimura K 1996 *Phys. Rev.* B **53** 2667
[32] Dynes R C, Narayanamurti V and Garno J P 1978 *Phys. Rev. Lett.* **41** 1509
[33] Chubukov A V and Eremin I 2010 *Phys. Rev.* B **82** 060504(R)
[34] Vorontsov A B and Vekhter I 2010 *Phys. Rev. Lett.* **105** 187004
Mazin I I, Devereaux T P, Analytis J G, Chu J H, Fisher I R, Muschler B and Hackl R 2010 *Phys. Rev.* B **82** 180502(R)
[35] Tanatar M A, Reid J P, Shakeripour H, Luo X G, Doiron-Leyraud N, Ni N, Bud'ko S L, Canfield P C, Prozorov R and Taillefer L 2010 *Phys. Rev. Lett.* **104** 067002
[36] Wang Z S, Wang Z Y, Luo H Q, Lu X Y, Zhu J, Li C H, Shan L, Yang H, Wen H H and Ren C 2012 *Phys. Rev.* B **86** 060508(R)